Materials Research Express

PAPER

Direct fabrication of C12A7 electride target and room temperature deposition of thin films with low work function

RECEIVED
1 November 2016

REVISED
13 February 2017

ACCEPTED FOR PUBLICATION
1 March 2017

PUBLISHED
23 March 2017

Wenwei Zou, Karim Khan, Xunna Zhao, Chaoting Zhu, Jinhua Huang, Jia Li, Ye Yang and Weijie Song

Ningbo Institute of Material Technology and Engineering, Chinese Academy of Sciences, Ningbo 315201, People's Republic of China

E-mail: lijia@nimte.ac.cn **and** weijiesong@nimte.ac.cn

Keywords: C12A7, electride, magnetron sputtering, work function

Abstract

In this work, a high density (94%) and high electron concentration (2.3×10^{20} cm^{-3}) doped C12A7 electride ceramic target for magnetron sputtering was prepared by directly heating the C12A7 nano powder to above its melting point. The effects of the temperature on the electron concentration was explored. Furthermore, a smooth ($R_q = 0.6$ nm), high transparent and low work function ($\Phi = 2.9$ eV) C12A7 electride thin film was deposited via magnetron sputtering. This result provides a suitable route for the fabrication of large-scale C12A7 electride film and has a bright prospect for application in optoelectronic devices.

1. Introduction

Low work function thin films have important significance in the application of electronic and optoelectronic devices [1] that require low work function and atmospheric stability, such as cathode materials in OLED [2] or new dopant-free carrier selectivity cells [3]. The inorganic $12CaO \cdot 7Al_2O_3$ (C12A7) electride is a new and excellent material that features low work function and room temperature stability at the same time [4, 5]. The unit cell of C12A7 electride consists of a positively charged $[Ca_{24}Al_{28}O_{64}]^{4+}$ framework together with trapped electrons in the framework to maintain electrical neutrality [6]. The unique crystal structure endows this high alumina cement to have excellent electrical properties with low work function (2.4 eV), metallic conduction with rather high electrical conductivity (1500 S cm^{-1}) and atmospheric stability as well [7].

So far, the fabrication method of the C12A7 electride thin films were mainly classified into two strategies. One is obtain an insulator C12A7 film by various techniques [8–13] and then reduce it into C12A7 electride film by different reduction processes. The insulator C12A7 thin films were first deposited at RT using pulsed laser deposition (PLD) [8–12] or chemical solution deposition (CSD) method [13]. The reduction processes include annealing the amorphous thin film at high temperatures in the H_2 atmosphere followed by ultraviolet light irradiation [8], hot implantation with Ar^+ ion fluencies [12], and a two-stage film deposition process combined with chemical mechanical polishing [14]. Although high electrical properties have been reported to result from the use of these processes, they can give rise to problems of complex operations and be restrained by the small size of the film that could be produced, which is unable to meet the needs of large-scale products.

The other fabrication approach for the deposition of C12A7 electride thin film is magnetron sputtering method [15–17], which can be used to obtain C12A7 electride film from the conductor target directly. Watanabe *et al* [18] deposited the amorphous C12A7 thin film via RF sputtering and integrated it into an OLED device to act as an effective electron injection layer. This approach is suitable for large-scale fabrication and has great prospects for application in optoelectronic devices. The key goal is identifying how to obtain a high-quality electride ceramic target. Kim *et al* [19] heated insulating C12A7 disks in a carbon crucible at 1000–1200 °C for 24 h in an N_2 atmosphere and obtained the electride with an electron concentration of about 8×10^{19} cm^{-3}. This process required a long time for reduction, and the thickness of the disk was less than 1 mm. The same group also melted the C12A7 powder in a carbon crucible at 1600 °C twice to form a transparent glass and crystallized it in an evacuated silica tube at 1000 °C [20]. The obtained polycrystalline C12A7 electride exhibits an electrical conductivity up to 5 S·cm^{-1}, but the fabrication method required a multi-step process. The further optimization of the synthetic process with which to prepare a C12A7 electride ceramic target with a high electron concentration is worthy of study.

In this work, we developed an improved preparation method for a dense and high electron concentration doped C12A7 ceramic target in which direct thermal heating of C12A7 nano powder to above its melting point in a carbon crucible in an inert atmosphere is used. The effects of heating temperatures on the electron concentration are explored. Furthermore, an amorphous C12A7 electride thin film was deposited at room temperature via magnetron sputtering using this home-made target. A low work function ($\Phi \approx 2.9$ eV) and smooth surface ($R_q \approx 0.6$ nm) film was obtained.

2. Experimental procedures

2.1. Synthese of C12A7 target

Undoped C12A7 powder was obtained by a conventional solid-state reaction from a stoichiometric mixture of analytical grade $CaCO_3$ (Aldrich) and Al_2O_3 (Sinopharm) (mole ratio of CaO: Al_2O_3 = 12: 7). The sample was placed in an agate tank and an appropriate amount of water was added, then ground the mixture for 4 h under a planetary ball mill (QM-3SP2, Instrument Factory of Nanjing University, China) with the speed of 300 RMP. The mixed powder was reacted in a Box-type resistance furnace (YFX12/16Q-YC, Shanghai Y-feng electrical furnace Co. Ltd, China) at 1250 °C for 8 h in air and then crushed in a agate mortar (Φ120 mm) to obtain fine powder. The powder was then divided into several parts and put into different carbon crucibles (ψ30 mm × 40 mm and ψ80 mm × 110 mm) with caps. Reduction process were carried out in a vacuum furnace (SQFL-1700, SIOMM, China) at different temperatures ranging from 1250 °C to 1500 °C in a flowing N_2 atmosphere and then cooled down at a rate of 10 °C/min. After thermal treatment, the powder turned into bulk form and the color changed from white to dark green. The bulk C12A7 material was then polished with grinding machine (KGS618, JIYE, China) into a smooth surface for subsequent sputtering process.

2.2. Film deposition

The C12A7 thin films were deposited on quartz glasses (30 mm × 30 mm, ~1 mm in thickness) and single crystal silicon (1 0 0) (30 mm × 30 mm, ~0.52 mm in thickness) substrates by magnetron sputtering (JCP-350M2, Ticono, Beijing, China) using the C12A7 target that fabricated as mentioned above. Before thin film deposition, the substrates were ultrasonically cleaned in deionized water, ethanol and acetone for 20 min respectively and then followed by nitrogen gas blowing. During deposition, RF powder was set at 200 W with Ar gas flow fixed at 30 sccm which was controlled by the mass flow controller. The substrate temperature was fixed at room temperature.

2.3. Characterization

The structure of the C12A7 powder and bulks were examined using x-ray diffraction (Bruker AXS/D8 advance XRD) with Cu Kα radiation (λ = 0.154 06 nm, 40 kV, 360 mA). The Raman spectrum of the samples were characterized by a micro-Raman spectrometer (Nanofinder, Tokyo Instruments) with the frequency-doubled CW-Nd:YAG laser light (λ = 532 nm). The optical properties of as-prepared samples were studied at room temperature by a UV–vis spectrophotometer (Perkin-Elmer, Lambda 950, USA). The infrared absorption band of the samples were examined by a Fourier transform infrared spectroscopy (FTIR, Nicolet 6700, Thermo, USA) using a KBr pressed disk. The morphology, microstructure of the target and composition analyses of the as-deposited film were performed using a field emission scanning electron microscopy (FE-SEM)/energy-dispersive x-ray analysis (EDAX) system (S-4800, Hitachi Ltd, Tokyo, Japan). The density of the samples was measured by the Archimedes method using a densitometer (MH-600, MatsuHaku, Taichung, Taiwan). The thickness of the film was measured by using spectroscopic ellipsometer (Woollam M-2000DI). The surfaces of the as-deposited thin films were examined by an atomic force microscopy (AFM, CSPM5500 Scanning Probe Microscopy). The photoelectron measurements were performed using Kratos AXIS ULTRADLD. The UPS spectra were recorded using a He I radiation ($h\nu$ = 21.22 eV) with a step size of 0.025 eV.

3. Results and discussion

3.1. C12A7 target

Figure 1(a) shows the XRD patterns of the C12A7 powder fabricated by solid-state reaction and those heated in carbon crucibles at different temperatures. The powder and samples heated below 1500 °C showed well-resolved sharp peaks in the XRD pattern, which were in good agreement with the well crystalline C12A7 phase (PDF#09-0413). No obvious distinction was observed with varied heating temperatures below 1500 °C. However, when the sample was heated to 1500 °C, it decomposed to CA + C3A. This phenomenon was reported by Sung Wng Kim [21] that O^{2-} ions in the framework tends to remove at high temperature, which lead to the decomposition of C12A7 phase into CA + C3A mixture. To further confirm the detailed structure and chemical composition of the heated samples, Raman spectrums of the samples after heating were characterized. The Raman spectrums of all the samples heated from 1250 °C to 1450 °C were nearly the same. Figure 1(b) shows the Raman spectrum

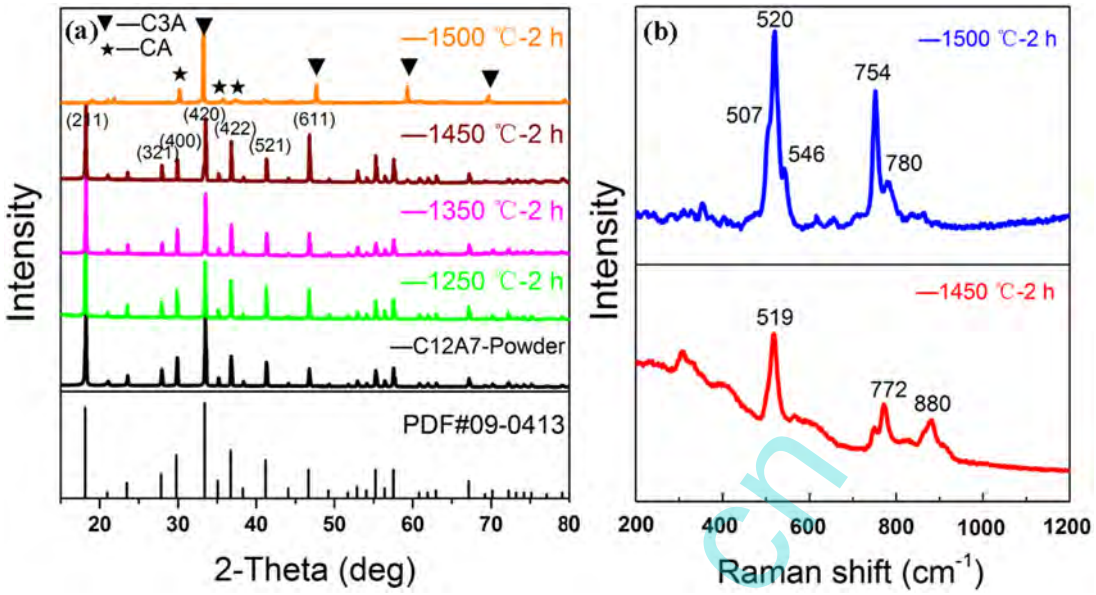

Figure 1. (a) XRD patterns of samples heated at different temperatures; (b) Raman spectrum of the samples heating at 1450 °C and 1500 °C for 2 h.

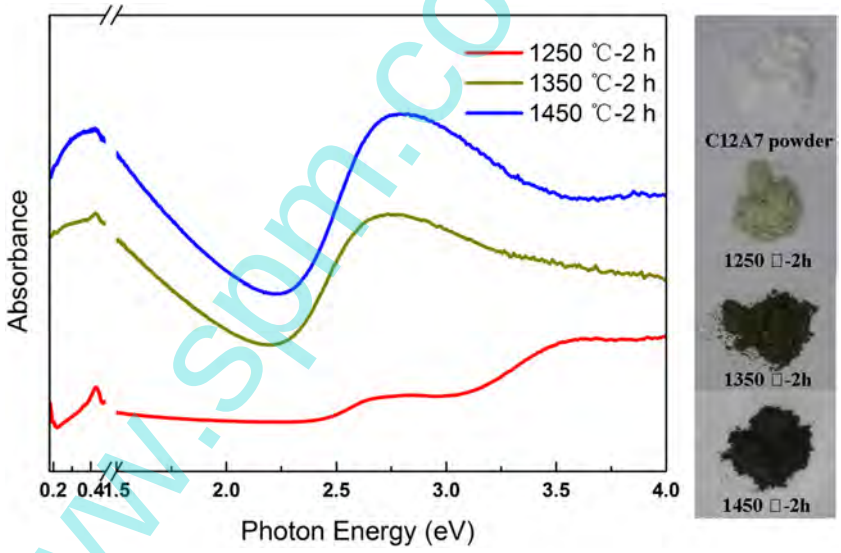

Figure 2. Optical absorption spectra of samples reduced at different temperature.

of the sample heating at 1450 °C and 1500 °C for 2 h, respectively. The intense peaks located at 519 cm^{-1} and 772 cm^{-1} were the characteristic peaks of C12A7 phase. The bands at 519 cm^{-1} and 772 cm^{-1} were origin from the framework Al–O vibrations and belonged to the totally symmetric modes [22]. While for the sample heated at 1500 °C, there were four obviously peaks at 520 cm^{-1}, 546 cm^{-1}, 754 cm^{-1}, 780 cm^{-1}, respectively. The peaks located at 546 cm^{-1} and 521 cm^{-1} were corresponding to the CA phase while the characteristic peaks of C3A phase were at 756 cm^{-1} and 508 cm^{-1} [23]. Combining the XRD patterns and the Raman spectrums, we could ensure that C12A7 bulks were pure phase at the heating temperature below 1500 °C, while tended to decompose into CA + C3A mix phase when the temperature higher than 1500 °C.

For the C12A7 electride, the change of the absorption spectrum is a direct embodiment of the electron concentration. Figure 2 shows the optical absorption spectra of the samples heated at different temperatures. Here, we use the UV–vis and Fourier transform infrared spectroscopy to determine the UV–vis absorption intensity and infrared absorption intensity, respectively. We crushed the reduced samples into fine powders. The intensities of the UV–vis absorption were estimated by Kubelka–Munk analysis of the diffuse reflectance spectra of powdered samples which are press onto a $BaSO_4$ reflected back. Because the $BaSO_4$ in the UV–vis region have little absorption, we can safely draw the conclusion that the absorption is caused by the C12A7 electride. We also crushed the samples into fine powders and diluted with KBr powder for the infrared absorption measurements. The reduction treatment induced two absorption bands at 2.8 and 0.4 eV, respectively, which indicated the electrons

Table 1. The electrons concentration of the reduced samples heated at different temperatures.

Temperature/°C	Time/h	Electrons concentration/cm^{-3}
1250	2	4.9×10^{19}
1350	2	2.1×10^{20}
1450	2	2.3×10^{20}

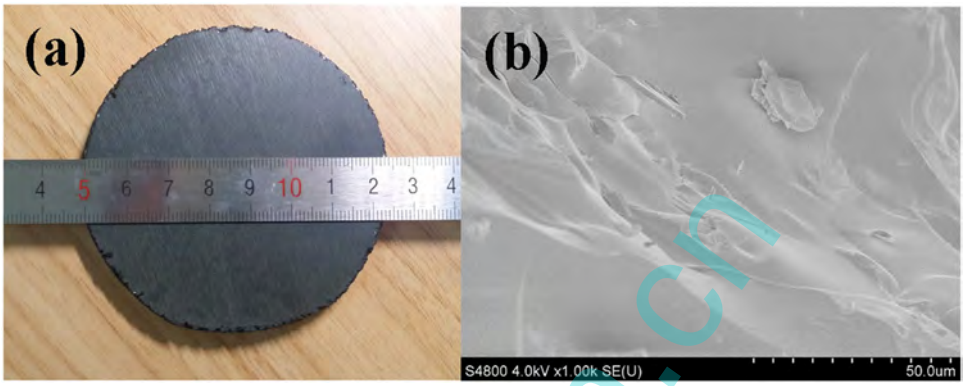

Figure 3. (a) Optical photograph and (b) cross-section SEM image of the target heated at 1450 °C.

were captured by the positively charged cage at the F^+-like center. The former absorption bands is attributed to the intracage electron transition to a 1p excited-state in the same cage which resulted in the green coloration. The latter is attributed to the intercage transition from the 1s ground state of the occupied cage to the 1s state in a neighboring empty cage [24]. The band shape and peak position of the two bands agree well with the results that published by Satoru Matsuishi [6]. The increase of the absorption intensity reflected the increase of the electron concentration. It showed that increase the heating temperature can increase the intensities of both bands which reflect the electron concentration. While as the temperature higher than the melting point (1290 °C) [21] of the C12A7 electride, further improve the heating temperature had little effect on the intensity incensement. At high temperature, the atmosphere inside the carbon crucible was a strongly reducing atmosphere. The reduction process was likely to be the joint actions of CO/CO_2 reduction process [19] and melt-solidification process [20].

Though we can observe the change of the electron concentration from the absorption spectra, the accurate electron concentration cannot be read from the spectra. The iodometry is a simple and accurate way to determine the concentration of electrons [25]. Parts of the bulks after reduction were further ground into powder form for iodometry measurement. Approximately 50 mg of each powered sample was placed in a conical flask. Aqueous I_2 solution (1.0×10^{-3} M, ~10 ml) was then poured into each vessel. The pH was adjusted to ~0.5 with HCl. The vessel was sealed to prevent the reoxidation of I^- ions by ambient oxygen, and the stirred solution was maintained at a temperature of 20 °C in a dark room. After confirming complete dissolution of the sample, the amount of residual I_2 was titrated using sodium thiosulfate solution (1.0×10^{-3} M). Observation of the endpoint was enhanced by adding three drops of starch solution. Each group of experiments were repeated for three times, taking the average of the experimental results. Table 1 shows the calculated concentration of the electrons in different samples. All the experiments are operated in the atmospheric environment, the real result maybe higher than that determined. Even though, the best result is higher than the reported results that reduced in carbon crucible [19].

The other key assessment criterion for the ceramic target is its density, which directly influence the rate and the quality of the magnetron sputtering. The density of the sample heated at 1450 °C was measured to be 2.49 g cm^{-3} according to the Archimedes principle and the relative density is calculated as high as 94%. The result showed that the high-density ceramic target was suitable for the magnetron sputtering. The optical photograph of the 3 inch target and the cross-section microscopic image with a scale bar of 50 μm are shown in figure 3. It was observed that the target is dark color with a smooth surface after mechanical polishing. The cross-section image of the target is dense and smooth, neither pores nor grain boundary could be observed.

3.2. C12A7 thin film

In this part, we deposited C12A7 thin film by magnetron sputtering method using the electride target to explore its potential applications in optoelectronic devices. The sputtering process was conducted at room temperature with the sputtering power set at 200 W. The measured thickness of the grown thin film was about 690 nm. Figure 4 shows the UV–Vis optical transmittance + reflectance spectrum of the as-deposited thin films before and after annealing compared with quartz substrate. It was denoted that the as-deposited thin film had almost no

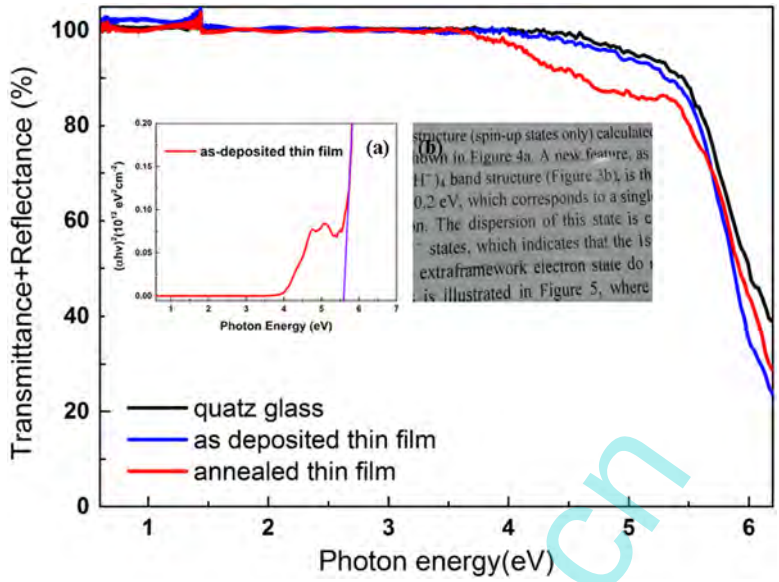

Figure 4. UV–Vis optical transmittance + reflectance spectrum of the C12A7 thin films before and after annealing compared with quartz substrate. The inset figure (a) is the $(\alpha h\upsilon)^2$ versus $h\upsilon$ plot of the as-deposited C12A7 thin film; (b) is the optical photograph of the as-deposited C12A7 thin film.

absorption at visible wavelength range. An obvious absorption band at 4.7 eV was observed for the as-deposited thin film, which might be caused by the electron spin-paired state [26]. Comparatively, it was observed that the absorption band disappeared after 700 °C annealing in air atmosphere. It was reported that C12A7 electride is stable below 600 °C and turn into insulator in the atmospheric environment at higher temperature [27]. The differences of the absorption band at 4.7 eV between the samples before and after annealing might be the supplementary proof of the existence of electron in the as-deposited thin film. The inset figure (b) shows the optical photograph of the as-deposited C12A7 thin film with a thickness about 690 nm, indicating that the film has a high transparent property. The band gap energy is a fundamental property of semiconductors, which indicates the threshold for the absorption of photons. The inset figure (a) shows the $(\alpha h\upsilon)^2$ versus $h\upsilon$ plot of the as-deposited film with the thickness of about 690 nm. The band gap energy of C12A7 electride thin film was calculated via Tauc's formula

$$\alpha = B\frac{(h\upsilon - E_g)^{1/r}}{h\upsilon} \tag{1}$$

where α is the absorption coefficient, E_g is the band gap energy, B is the proportionality constant, $h\upsilon$ is the photon energy in eV, and $r = 1/2$ indicating the allowed direct transition of C12A7 electride film [8]. The band gap value of the C12A7 thin film that got from the intersection of tangent and transverse coordinates was about 5.6 eV, which fit well with the band gap value from cage conduction band to valence band that reported by Satoru Matsuishi [28].

The surface roughness of the film has a great effect on the device performance. In order to observe surface topography of the C12A7 electride thin films, AFM images of the 690 nm C12A7 thin film with a scan area of $2 \times 2\ \mu m^2$ are presented in figure 5(a). The as-deposited thin film was dense without evident particles or clusters. The surface root mean square roughness (R_q) was calculated to be 0.6 nm. It indicated that the C12A7 thin film had a smooth surface and was suitable for the device application. The XRD pattern of the as-deposited thin film revealed an amorphous structure, which was not shown here. To further investigate the composition of the as-deposited film, we deposited the film on a single crystal silicon substrate via sputtering, the EDX testing result is shown in figure 5(b). The atomic ratio of Ca/Al derived from EDX was approximately 12:15 which in the range of allowable error. As a result, it can be deduced that sputtering process would not change the stoichiometric ratio of the target and the as-deposited film was amorphous C12A7 thin film.

The low work function is another remarkable characteristic of the C12A7 electride. Figure 6 shows the UPS spectra of the target prepared at 1450 °C for 2 h and the thin film deposited at room temperature. The insert figure is the enlarged cutoff regions of the samples. For the target and the thin film, the secondary electron cutoff energy values were about 2.4 eV and 2.9 eV, respectively. The low work function was near to the LiF/Al thin film which is wildly used in the OLED device. The C12A7 electride is a low work function material and stable in the atmospheric environment, which will find more prominent applications in the optoelectronic devices.

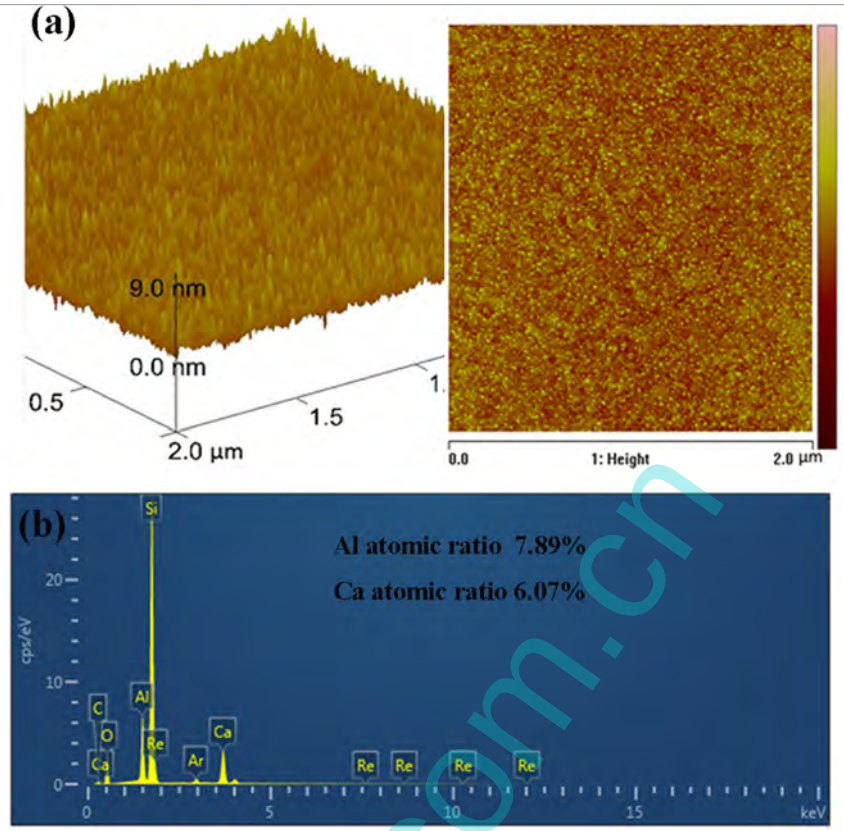

Figure 5. (a) AFM image and (b) EDX atom composition of the as-deposited thin film.

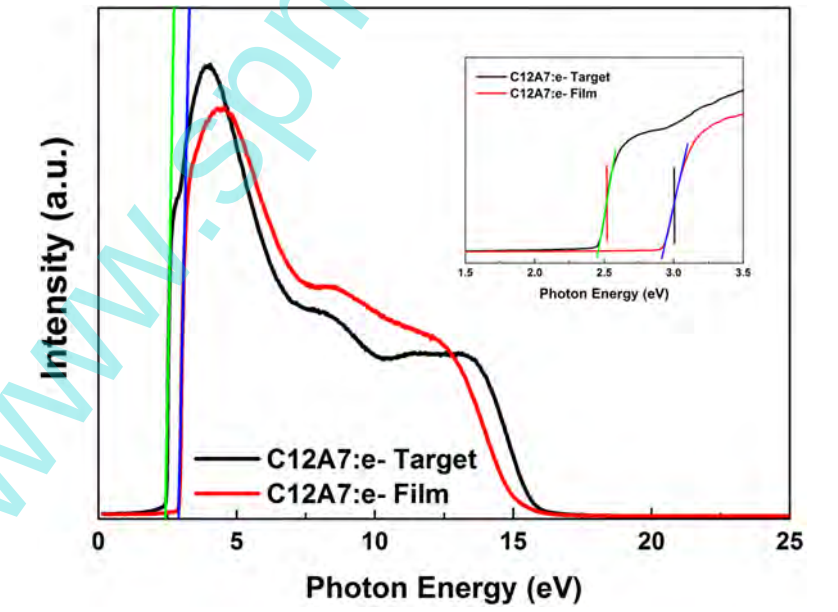

Figure 6. UPS spectra of the C12A7 electride target and the sputtering thin film. The inset image was the enlarged cutoff regions of the samples.

4. Conclusions

In this work, we explored the change of the electron concentration in the C12A7 electride target at different heating temperatures near its melting point. By optimizing the reduction condition, the maximum electron concentration of 2.3×10^{20} cm^{-3} was obtained for the C12A7 powder heated at 1450 °C for 2 h and the 3 inch size electride target has a relative density of 94% was achieved. Furthermore, a smooth ($R_q = 0.6$ nm) and low work function (2.9 eV) amorphous thin film was prepared using the home-made target via magnetron sputtering process. For the optoelectronic devices application, an additional investigation is currently underway.

Acknowledgments

This work was supported by National Natural Science Foundation of China (61574144), Zhejiang Natural Science Foundation (LY15F040004), the program for Ningbo Municipal Science and Technology Innovative Research Team (2015B11002) and International S&T Cooperation Program of China (ISTCP) (2015DFH60240).

References

[1] Kamiya T and Hosono H 2005 Creation of new functions in transparent oxides utilizing nanostructures embedded in crystal and artificially encoded by laser pulses *Semicond. Sci. Technol.* **20** S92–102
[2] Yanagi H, Kim K-B, Koizumi I, Kikuchi M, Hiramatsu H and Miyakawa M 2009 Low threshold voltage and carrier injection properties of inverted organic light-emitting diodes with $[Ca_{24}Al_{28}O_{64}]^{4+}(4e^-)$ cathode and $Cu_{2-x}Se$ anode *J. Phys. Chem.* C **113** 18379–84
[3] Bullock J, Hettick M and Geissbühler J 2016 Efficient silicon solar cells with dopant-free asymmetric heterocontacts *Nat. Eng.* **1** 15031
[4] Hayashi K, Matsuishi S, Kamiya T, Hirano M and Hosono H 2002 Light-induced conversion of an insulating refractory oxide into a persistent electronic conductor *Nature* **419** 462–5
[5] Toda Y, Yanagi H, Ikenaga E, Kim J J, Kobata M and Ueda S 2007 Work function of a room-temperature, stable electride $[Ca_{24}Al_{28}O_{64}]^{4+}(4e^-)$ *Adv. Mater.* **19** 3564–9
[6] Matsuishi S, Toda Y, Miyakawa M, Hayashi K, Kamiya T and Hirano M 2003 High-density electron anions in a nanoporous single crystal: $[Ca_{24}Al_{28}O_{64}]^{4+}(4e^-)$ *Science* **301** 626–9
[7] Kim S W, Matsuishi S, Nomura T, Kubota Y, Takata M and Hayashi K 2007 Metallic state in a lime-alumina compound with nanoporous structure *Nano Lett.* **7** 1138–43
[8] Toda Y, Miyakawa M, Hayashi K, Kamiya T, Hirano M and Hosono H 2003 Thin film fabrication of nano-porous $12CaO \cdot 7Al_2O_3$ crystal and its conversion into transparent conductive films by light illumination *Thin Solid Films* **445** 309–12
[9] Nishio Y, Nomura K, Miyakawa M, Hayashi K, Yanagi H and Kamiya T 2008 Fabrication and transport properties of $12CaO \cdot 7Al_2O_3$ (C12A7) electride nanowire *Phys. Status Solidi* a **205** 2047–51
[10] Nishio Y, Nomura K, Yanagi H, Kamiya T, Hirano M and Hosono H 2010 Short-channel nanowire transistor using a nanoporous crystal semiconductor $12CaO \cdot 7Al_2O_3$ *Mater. Sci. Eng.* B **173** 37–40
[11] Miyakawa M, Ueda N, Kamiya T, Hirano M and Hosono H 2007 Novel room temperature stable electride $12SrO \cdot 7Al_2O_3$ thin films: fabrication, optical and electron transport properties *J. Ceram. Soc. Japan* **115** 567–70
[12] Miyakawa M, Toda Y, Hayashi K, Hirano M, Kamiya T and Matsunami N 2005 Formation of inorganic electride thin films via site-selective extrusion by energetic inert gas ions *J. Appl. Phys.* **97** 023510
[13] Zahedi M, Ray A K and Barratt D S 2008 Preparation and crystallization of sol–gel C12A7 thin films *J. Phys. D: Appl. Phys.* **41** 035404
[14] Miyakawa M, Hirano M, Kamiya T and Hosono H 2007 High electron doping to a wide band gap semiconductor $12CaO \cdot 7Al_2O_3$ thin film *Appl. Phys. Lett.* **90** 182105
[15] Jung C H, Hwang I R, Park B H and Yoon D H 2013 Characterization of $12CaO \cdot 7Al_2O_3$ doped indium tin oxide films for transparent cathode in top-emission organic light-emitting diodes *J. Nanosci. Nanotechnol.* **13** 7556–60
[16] Jung C H, Tai P H, Kang Y K, Jang D S and Yoon D H 2008 $12CaO \cdot 7Al_2O_3$ doped indium-tin-oxide thin film for transparent cathode in organic light-emitting devices *Surf. Coat. Technol.* **202** 5421–4
[17] Tai P H, Jung C H, Kang Y K and Yoon D H 2009 Electrical and optical properties of $12CaO \cdot 7Al_2O_3$ electride doped indium tin oxide thin film deposited by RF magnetron co-sputtering *Thin Solid Films* **517** 6294–7
[18] Watanabe S, Watanabe T, Ito K and Miyakawa N 2013 Electron injecting material for OLEDs driven by oxide TFTs: amorphous C12A7 electride *SID Symp. Digest Tech. Pap.* **44** 1473–6
[19] Kim S-W, Hayashi K, Hirano M, Hosono H and Tanaka I 2006 Electron carrier generation in a refractory oxide $12CaO \cdot 7Al_2O_3$ by heating in reducing atmosphere: conversion from an insulator to a persistent conductor *J. Am. Ceram. Soc.* **89** 3294–8
[20] Kim S W, Miyakawa M, Hayashi K, Sakai T, Hirano M and Hosono H 2005 Simple and efficient fabrication of room temperature stable electride: melt-solidification and glass ceramics *J. Am. Ceram. Soc.* **127** 1370–1
[21] Kim S W and Hosono H 2012 Synthesis and properties of $12CaO \cdot 7Al_2O_3$ electride: review of single crystal and thin film growth *Phil. Mag.* **92** 2596–628
[22] Kajihara K, Matsuishi S, Hayashi K, Hirano M and Hosono H 2007 Vibrational dynamics and oxygen diffusion in a nanoporous oxide ion conductor $12CaO \cdot 7Al_2O_3$ studied by O-18 labeling and micro-Raman spectroscopy *J. Phys. Chem.* C **111** 14855–61
[23] Ruszak M, Witkowski S, Pietrzyk P, Kotarba A and Sojka Z 2011 The role of intermediate calcium aluminate phases in solid state synthesis of mayenite ($Ca_{12}Al_{14}O_{33}$) *Funct. Mater. Lett.* **4** 183–6
[24] Sushko P V, Shluger A L, Hayashi K, Hirano M and Hosono H 2003 Hopping and optical absorption of electrons in nano-porous crystal $12CaO \cdot 7Al_2O_3$ *Thin Solid Films* **445** 161–7
[25] Yoshizumi T, Matsuishi S, Kim S-W, Hosono H and Hayashi K 2010 Iodometric determination of electrons incorporated into cages in $12CaO \cdot 7Al_2O_3$ crystals *J. Phys. Chem.* C **114** 15354–7
[26] Kim S W, Shimoyama T and Hosono H 2011 Solvated electrons in high-temperature melts and glasses of the room-temperature stable electride $[Ca_{24}Al_{28}O_{64}]^{4+} \cdot 4e^-$ *Science* **333** 71–4
[27] Miyakawa M, Hayashi K, Hirano M, Toda Y, Kamiya T and Hosono H 2003 Fabrication of highly conductive $12CaO \cdot 7Al_2O_3$ thin films encaging hydride ions by proton implantation *Adv. Mater.* **15** 1100–5
[28] Matsuishi S, Kim S W, Kamiya T, Hirano M and Hosono H 2008 Localized and delocalized electrons in room-temperature stable electride $[Ca_{24}Al_{28}O_{64}]^{4+}(O^{2-})_{2-x}(e^-)_{2x}$: analysis of optical reflectance spectra *J. Phys. Chem.* C **112** 4753–60